Calculation of Dehumidification Coefficients for Numerical Simulation of Desiccant Wheel

Yoshihisa MOMOI[1], Ryuichiro YOSHIE[2], Akira SATAKE[3], and Hiroshi YOSHINO[4]

[1] Division of Global Architecture, Graduate School of Engineering, Osaka University, Japan

[2] Department of Architecture, Graduate School of Engineering, Tokyo Polytechnic University, Japan

[3] Maeda Corporation, Tokyo, Japan

[4] Department of Architecture and Building Science, Graduate School of Engineering, Tohoku University, Japan

Abstract

In the previous study, a numerical method which simulates combined heat and moisture transfer process in solid desiccant materials was investigated. The calculation results successfully reproduced the cyclic process of the moisture adsorption and desorption. The validity of the numerical simulation method for the desiccant wheel was examined by the comparison between the experiment and the numerical simulation of the desiccant dehumidifier.

In this paper, it reports that the dehumidification performance of the desiccant wheel could be expressed as two dehumidification coefficients (*effectivenesses of the dehumidifier*) *in the psychrometric chart, from the result of the air temperature and humidity before and behind the desiccant wheel. One is effectiveness for relative humidity, another one is effectiveness for enthalpy.*

It was shown that the average temperature and humidity of the wheel outlet air were predictable without depending on the regeneration air temperature by using the effectivenesses of the dehumidifier.

Keywords: *Desiccant, Dehumidification, Numerical Simulation, Adsorption, Desorption*

Introduction

Desiccant dehumidifiers can remove moisture from air by using desiccant materials (absorbents such as silica gel), without cooling the air below its dew point. As the desiccant material absorbs moisture, it becomes saturated with water. Therefore, the desiccant material must be regenerated periodically. The regeneration air is heated to lower its relative humidity and dries the desiccant materials. In the case of a rotary wheel desiccant dehumidifier, a portion is being regenerated while the remainder is absorbing water for operating adsorption and regeneration at the same time. The wheel rotates between the adsorption part and the regeneration part.

In the previous reports [1, 2], the authors developed a numerical model of a desiccant wheel, derived the heat and moisture transport equations for the inside of the desiccant element. In addition, the authors measured equilibrium moisture content and moisture transfer coefficient, which are important parameters that determine the dehumidification performance. Moreover, numerical analysis inputting these measured values was conducted, and the validity of the numerical analysis was discussed, by comparing the calculation results with the experimental results of a desiccant system. This paper expresses the dehumidification performance of a desiccant wheel with two dehumidification coefficients (effectivenesses of the dehumidifier), by finding out the moisture absorption and desorption phenomena in the desiccant wheel. A

simplified numerical method for predicting the temperature and humidity of the air at the outlet of a desiccant wheel is discussed.

1. Heat and moisture transport equations in the desiccant wheel

As shown in Fig. 1, a desiccant wheel is cylindrical, and its cross-section has a corrugated honeycomb structure. Cutting out an infinitesimal volume from the wheel, a numerical model was produced with reference to the theory of the simultaneous transfer of heat and moisture proposed by Matsumoto [3] and Hokoi et al.

(1) Moisture balance equation for the air of the flow passage in the infinitesimal volume

$$\beta\rho_a \frac{\partial X_a}{\partial t} = -\beta u \rho_a \frac{\partial X_a}{\partial x} + \beta \frac{\partial}{\partial x}\left(\lambda_a ' \frac{\partial X_a}{\partial x} \right) - \gamma \frac{\partial w}{\partial t} \qquad \text{(Eq. 1)}$$

(2) Heat balance equation for the air of the flow passage in the infinitesimal volume

$$\beta C_a \rho_a \frac{\partial \theta_a}{\partial t} = -\beta u \rho_a C_a \frac{\partial \theta_a}{\partial x} + \beta \frac{\partial}{\partial x}\left(\lambda_a \frac{\partial \theta_a}{\partial x} \right) - \alpha S\left(\theta_a - \theta_d \right) \qquad \text{(Eq. 2)}$$

(3) Heat balance equation for the desiccant material in the infinitesimal volume

$$\begin{aligned} \left(1-\beta\right) C_d \rho_d \frac{\partial \theta_d}{\partial t} = \left(1-\beta\right) \frac{\partial}{\partial x}\left(\lambda_d \frac{\partial \theta_d}{\partial x} \right) \\ + L\alpha ' S\left(X_a - X_b \right) + \alpha S\left(\theta_a - \theta_d \right) \end{aligned} \qquad \text{(Eq. 3)}$$

The moisture content of the desiccant material varies according to the moisture transfer, which is induced by the difference in absolute humidity between the desiccant material surface and the air of the flow passage. Accordingly, it can be expressed by Eq. 4.

$$\gamma \frac{\partial w}{\partial t} = \alpha' S\left(X_a - X_b\right) \quad \text{(Eq. 4)}$$

The above equation system has four equations and five variables X_a, X_b, θ_a, θ_d, and w, and so the equation system is not closed. Then, the system is closed by assuming the local equilibrium in which the absolute humidity and moisture content of the desiccant material surface immediately follow the equilibrium moisture content curve as expressed by Eq. 5.

$$w = f\left(X_a, \theta_a\right) = f\left(X_b\ , \theta_d\right) \quad \text{(Eq. 5)}$$

where it is assumed that there is no heat loss, air flow is laminar, pressure and flow rate are constant, and temperature and moisture content are homogeneous in the thickness direction of the desiccant material.

2. State variation of the desiccant material during the absorption and desorption processes

Based on the calculation results with the above mentioned numerical calculation model for a desiccant wheel, phenomena that occur in the desiccant wheel during the absorption and

desorption processes is discussed. As shown in Fig. 2, the desiccant wheel was divided into 20 parts in the flow direction for calculation. Calculation was conducted for the adsorption and desorption processes. In the adsorption process, the air with a temperature of 30 degrees Celsius and a relative humidity of 90 % flows from the left side. These values were given as boundary conditions in the left ends of the computational domain. In the desorption process, the air with a temperature of 70 degrees Celsius and a relative humidity of 6.4 % flows from the right side. It was assumed that wheel thickness was 100 mm, moisture transfer coefficient $\alpha'S$ was 3.5, rotational speed was 30 rpm, and air velocity u was 1.16 m/s (which corresponds to the air velocity when 100 m^3/h of air passes through a wheel with a diameter of 300 mm).

The moisture content of the desiccant element changes along the curve of the equilibrium moisture content expressed by Eq. 5, according to the relative humidity at the element surface. Fig. 3 shows the change in moisture content with time at the divided elements x = 1, 10, 20 during the absorption process. Fig. 4 shows the change in the moisture content distribution with time in the thickness direction of the wheel. When the rotational speed of the wheel is 30 rpm, the variation in the moisture content in each element is not so large. Accordingly, it can be concluded that in order to improve the absorption performance, it is important to use a material whose equilibrium moisture content curve has a large gradient and a material whose dehumidification speed is high, that is, moisture transfer coefficient $\alpha'S$ is large.

3. State variation of the air passing through the desiccant wheel during the absorption and desorption processes

This section is focused on the state variation of the air that is dehumidified and humidified by the desiccant wheel. The air passing through the wheel follows the psychrometric chart. When OA passes through the desiccant wheel in the adsorption process, the latent heat of the water vapor adsorbed by the desiccant material emerges as sensible heat. That means the heat of adsorption is generated with the phase change, as shown in Fig. 5. Accordingly, temperature and humidity vary along the isenthalpic line in theory. However, the desiccant wheel is actually exposed to the high-temperature RA until just before the dehumidification process, and so the heat transfer from the regeneration side to the adsorption side occurs. Therefore, the average temperature and humidity of SA at the outlet of the adsorption side become higher than those of the ideal isenthalpic process. In theory, the relative humidity of the dehumidified air SA is equal to that of RA, but in reality, the relative humidity of SA changes with time. It is because the amount of water vapor that can be absorbed by the desiccant material is finite, and the desiccant material becomes saturated with water. Accordingly, actual SA undergoes a different state variation from an ideal process. The state variation of the air in the desorption side is also different from the ideal process. This was also demonstrated by the results of the experiment carried out at Tohoku University.

4. Definition of dehumidification effectiveness

The ideal process for adsorption is shown on the psychrometric coordinates in Figs. 6 and 7. Process air enters the dehumidifier at a state designated by OA, is ideally warmed and dehumidified along the isenthalpic line, exiting the humidifier at the air state labeled SA(ideal). However, as mentioned above, the adsorption and desorption processes are not isenthalpic in reality because the process air and the desiccant material can't be completely dried in a rotary system. Thus, the dehumidification effectivenesses ε_{F1} and ε_{F2} can be expressed as deviation from the ideal process by the following equations [4].

$$\varepsilon_{F1} = \frac{F1_{SA} - F1_{OA}}{F1_{RA} - F1_{OA}} \quad \text{(Eq. 6)}$$

$$\varepsilon_{F2} = \frac{F2_{SA} - F2_{OA}}{F2_{RA} - F2_{OA}} \quad \text{(Eq. 7)}$$

where enthalpy and relative humidity are expressed with the coordinate variables $F1$ and $F2$ in the psychrometric chart. The dehumidification effectiveness for enthalpy ε_{F1} is defined as proportion of the difference between the enthalpy coordinate of SA ($F1_{SA}$) and OA ($F1_{OA}$) to the difference between that of RA ($F1_{RA}$) and OA ($F1_{OA}$). The dehumidification effectiveness for relative humidity ε_{F2} is defined as proportion of the difference between the relative humidity coordinate of SA ($F2_{SA}$) and OA ($F2_{OA}$) to the difference between that of RA

($F2_{RA}$) and OA ($F2_{OA}$). The dehumidification performance increases as ε_{F1} becomes smaller and ε_{F2} becomes larger.

Coordinate transformation is expressed by the following equations, as derived by Jurinak [5] for silica gel desiccant:

$$F1 = -\frac{2865}{T^{1.490}} + 4.344X^{0.8624} \quad \text{(Eq. 8)}$$

$$F2 = \frac{T^{1.490}}{6360} - 1.127X^{0.07969} \quad \text{(Eq. 9)}$$

where T is absolute temperature [K], and X is absolute humidity [kg-H_2O/kg-Dry air].

5. Calculation of dehumidification effectiveness

5.1 Dehumidification effectiveness calculated from the experiment results

Fig. 8 shows the measured variations in temperature and relative humidity at the outlet. When rotational speed is low (at 5 rph), heat transfer from the desorption side to the adsorption side is little and the air undergoes the isenthalpic change as a whole, and so ε_{F1} becomes small. However, the relative humidity of SA is as high as about 26%, and ε_{F2} becomes about 0.6, although ideal ε_{F2} is 1.0. On the other hands, when rotational speed is high (at 60 rph), the

relative humidity of SA decreases to 7.5 %, and so ε_{F2} becomes as high as about 0.9. However, the behavior of air deviates from the isenthalpic line, and ε_{F1} becomes large.

Figs. 9 and 10 show ε_{F1} and ε_{F2} calculated from the experiment results of Tohoku University, respectively. As regeneration temperature increases, ε_{F1} and ε_{F2} decrease slightly. As air flow rate increases from 100 m^3/h to 200 m^3/h, ε_{F1} decreases by about 0.1. This is considered because the heat transferred from the desorption side to the adsorption side is purged immediately when the air flow rate is large. In addition, as air flow rate increases, the relative humidity of SA becomes higher, and so ε_{F2} decreases.

5.2 Dehumidification effectiveness calculated with the numerical calculation model

By conducting the calculation with the numerical calculation model for a desiccant wheel, it is possible to calculate dehumidification effectivenesses under a broad range of conditions. Figs. 11 and 12 show the calculation results of the dehumidification effectivenesses under the assumption that wheel thickness is 100 mm, the temperature and relative humidity of OA are 30 degrees Celsius and 16.0 g-H_2O/kg-Dry air, and the temperature and relative humidity of RA are 60, 70, or 80 degrees Celsius and 16.0 g-H_2O/kg-Dry air. The dehumidification effectivenesses calculated from the numerical simulation don’t vary significantly according to

regeneration temperature as well as the experiment. As air flow rate increases, both of ε_{F1} and ε_{F2} decrease.

6. Conclusions

Based on the results of the calculation with the numerical calculation model for a desiccant wheel, the spatial distribution and time variation of the moisture content for the desiccant material and the variations in air temperature and relative humidity at the outlet of the desiccant wheel are clarified. And then it is indicated that by analyzing the variations in air temperature and relative humidity before and behind the desiccant wheel with dehumidification effectivenesses, it is possible to easily estimate the air temperature and relative humidity at the outlet of the desiccant wheel. For the future, dehumidification effectivenesses will be further generalized for air flow rate and rotational speed.

Acknowledgments

The authors gratefully acknowledge the New Energy and Industrial Technology Development Organization (NEDO) of Japan through the Project of Solar Energy and New System Technology Resources and Development for funding this research with contract number

05002503-0. Research members include Prof. Mochida, Dr. Takaki, Dr. Lun, Dr. Yonekura, Mr. Enteria (Tohoku University), Mr. Kawahara, Mr. Kubo (Maeda Corporation), Dr. Mitamura (Ashikaga Institute of Technology) and Mr. Baba (Earth Clean Tohoku).

References

1. Yoshie, R., Momoi, Y., Satake, A., Yoshino, H. and Mitamura, T., Numerical Analysis of Heat and Moisture Transfer in Desiccant Wheel for Dehumidification, Proceedings of Clima 2007 WellBeing Indoors Abstract Book, p.531, 2007.

2. Momoi, Y., Yoshie, R., Satake, A., Yoshino, H. and Mitamura, T., Performance Prediction of Rotary Desiccant Wheel, Proceedings of the 29th AIVC Conference, Volume3, pp.297-302, 2008.

3. Matsumoto, M., Simultaneous Heat and Moisture Transfer in Porous Wall and Analysis of Internal Condensation, Energy Conservation in Heating, Cooling, and Ventilating Buildings, Proceedings of 1977 International Seminar of Heat and Mass Transfer, Dubrounik, Vol.1, pp.45-58, 1978.

4. TRNSYS 16.1 User's Manual, 2006.

5. Jurinak, J.J., Open Cycle Desiccant Cooling – Component Models and System Simulations, PhD Thesis, University of Wisconsin, Madison, 1982.

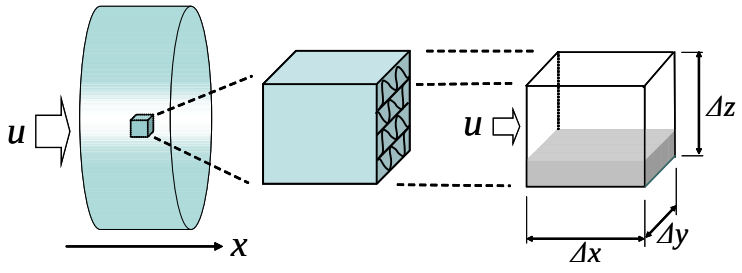

Fig. 1 Modeling of rotary wheel desiccant dehumidifier

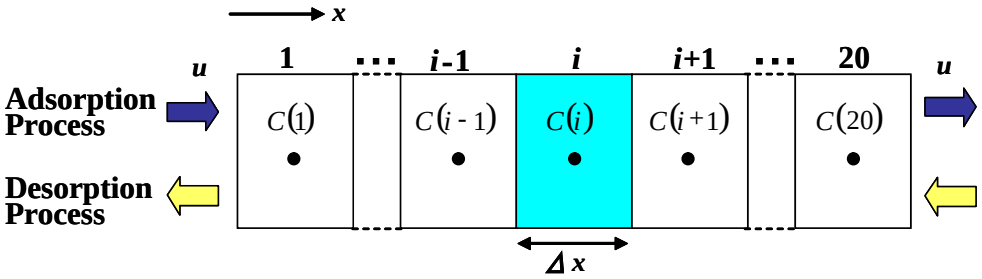

Fig. 2 Divided cells and boundary conditions

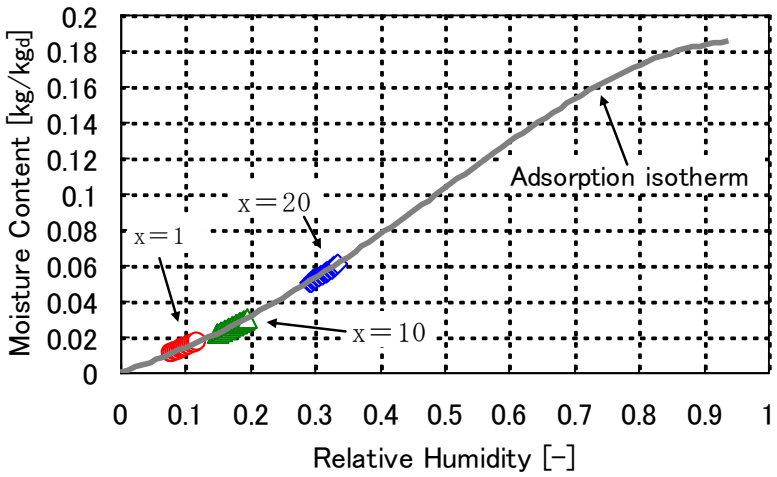

Fig. 3 State variation of the desiccant material on the absorption isotherm

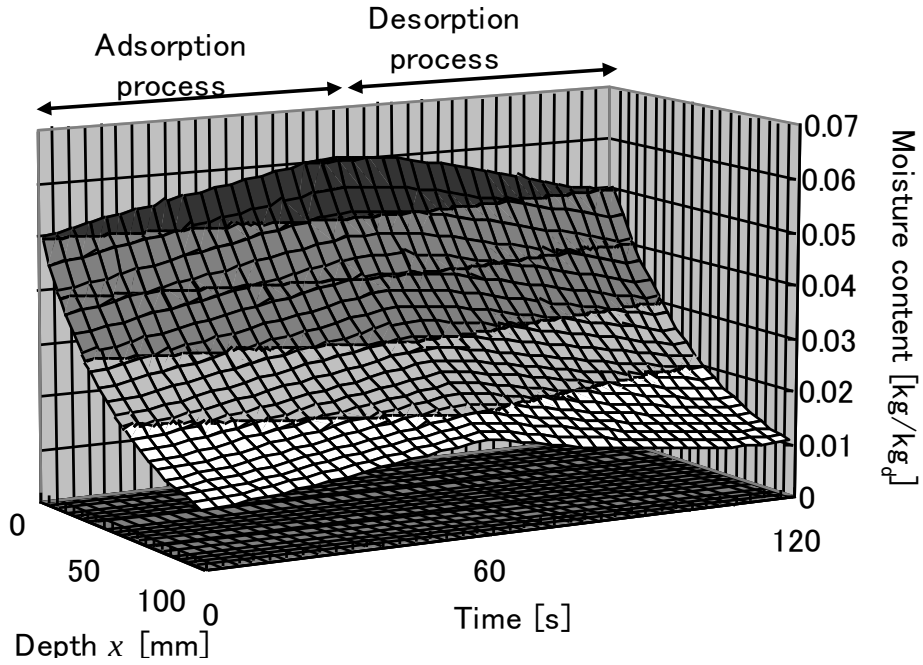

Fig. 4 Time variation of moisture content distribution

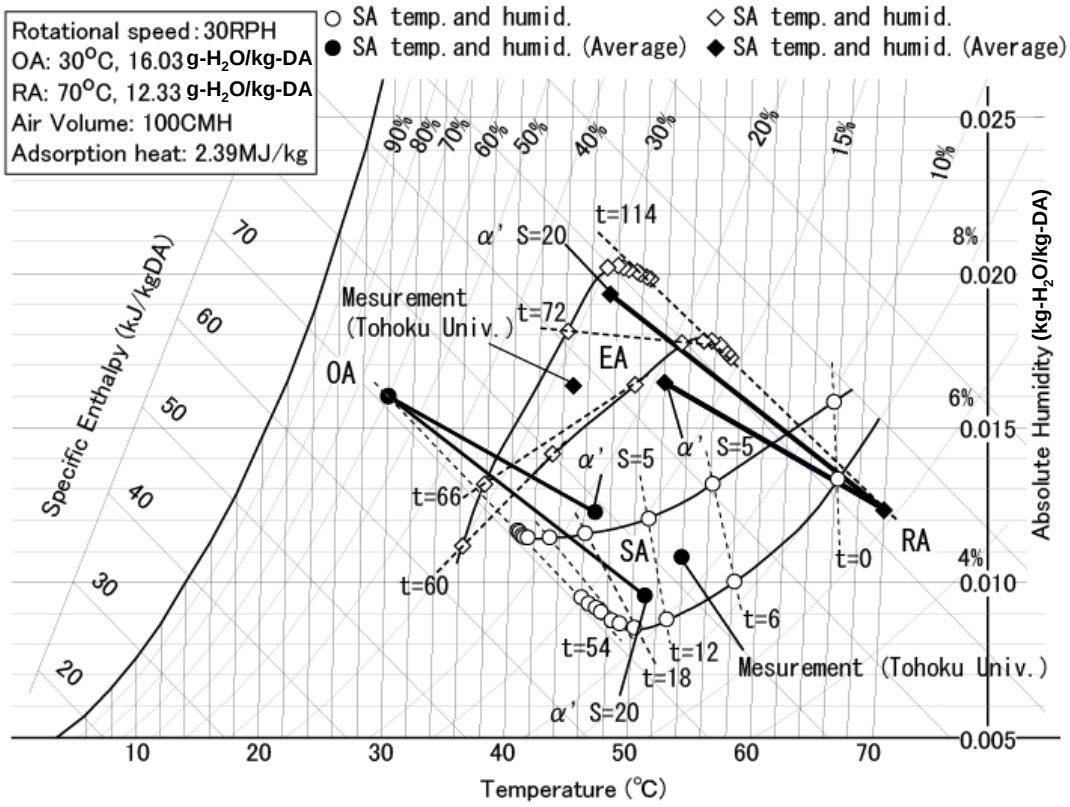

Fig. 5 Air temperature and humidity through the desiccant wheel

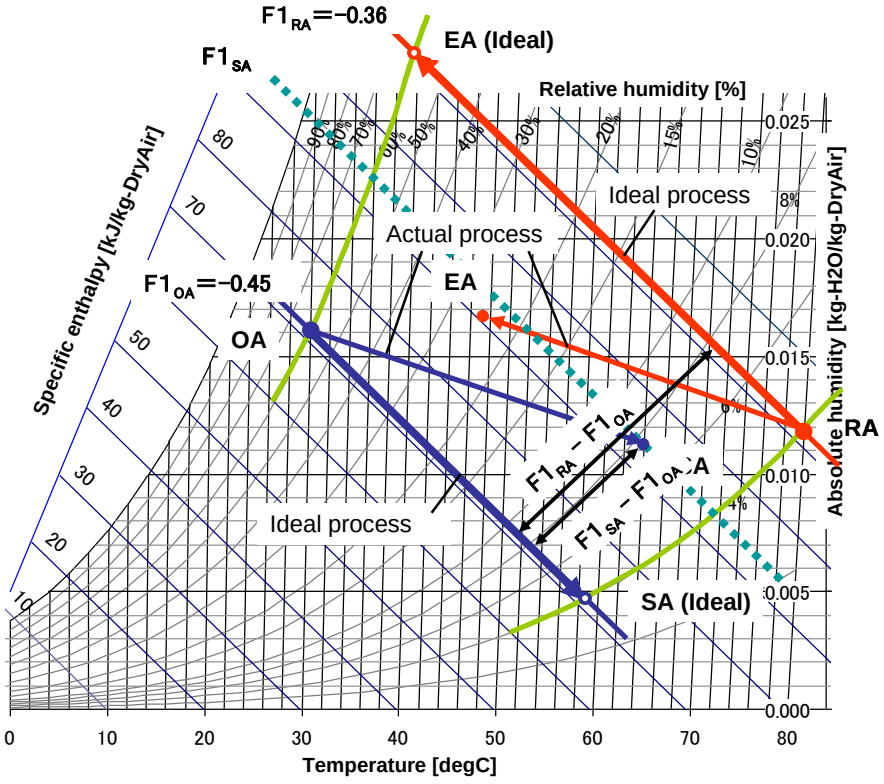

Fig. 6 Dehumidification effectiveness for enthalpy

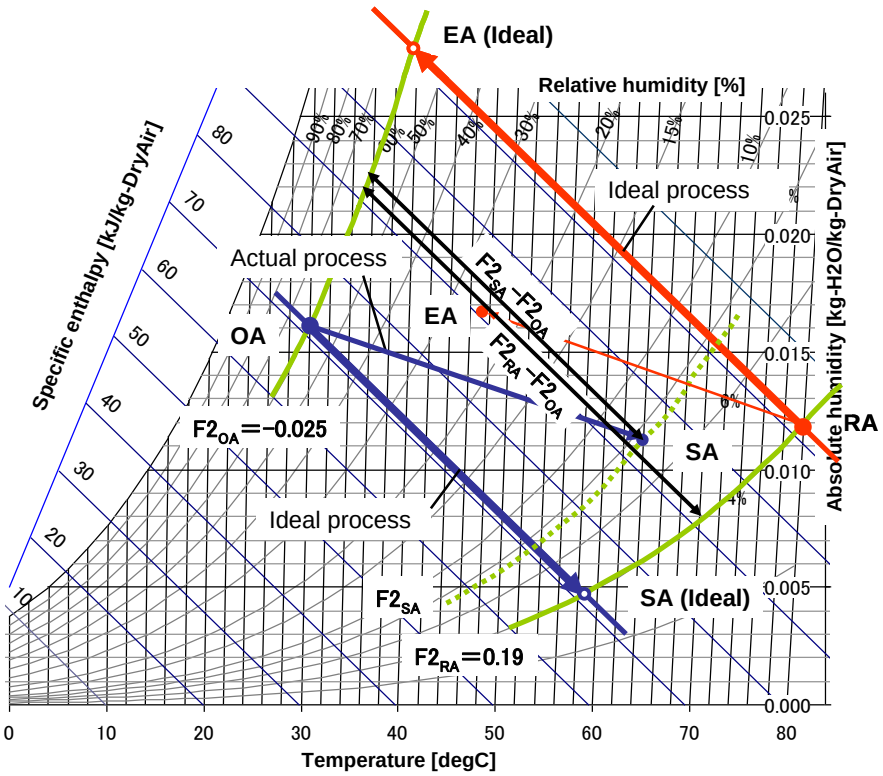

Fig. 7 Dehumidification effectiveness for RH

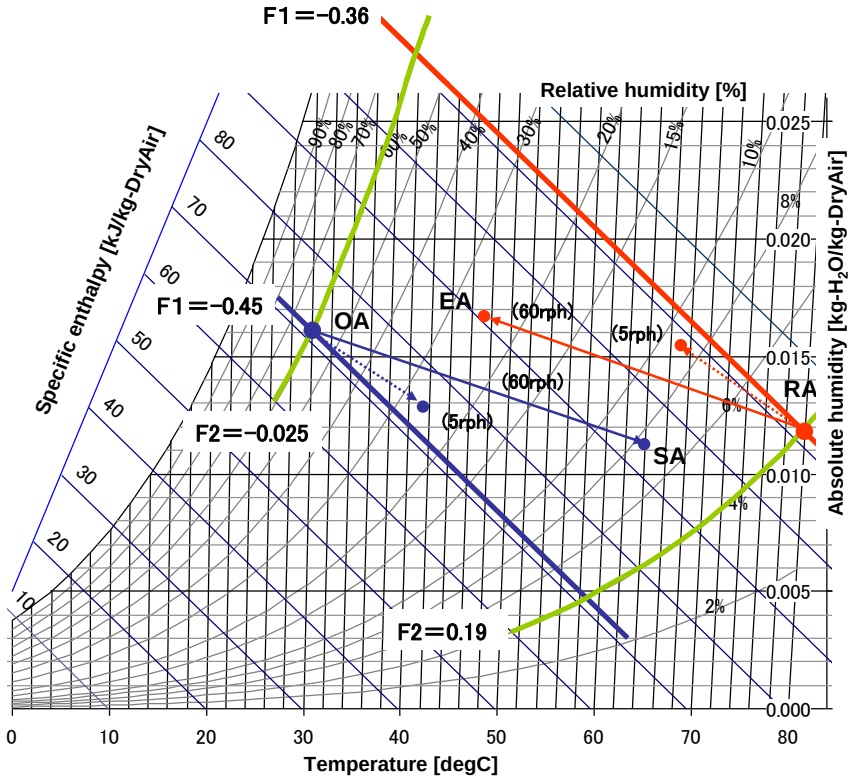

Fig. 8 Effect of rotational speed on humidification effectiveness

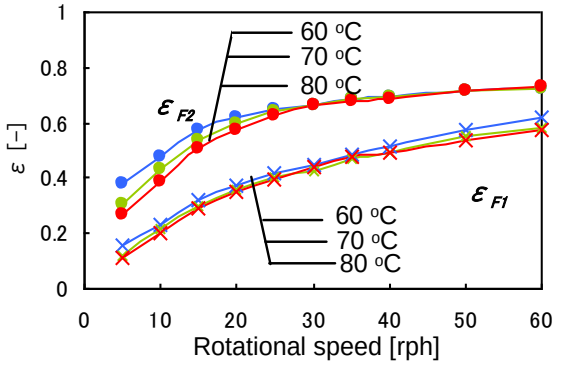

Fig. 9 Relation of rotational speed and dehumidification effectiveness (100 m^3/h)

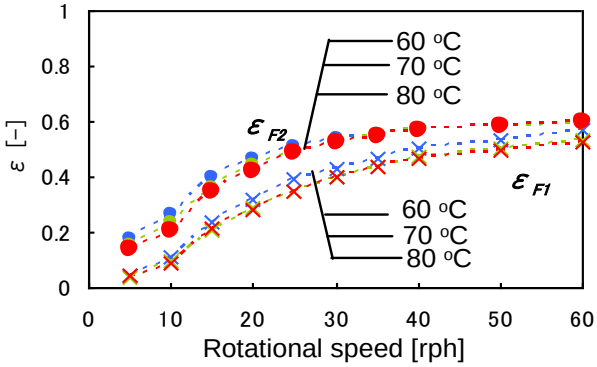

Fig. 10 Relation of rotational speed and dehumidification effectiveness (200 m^3/h)

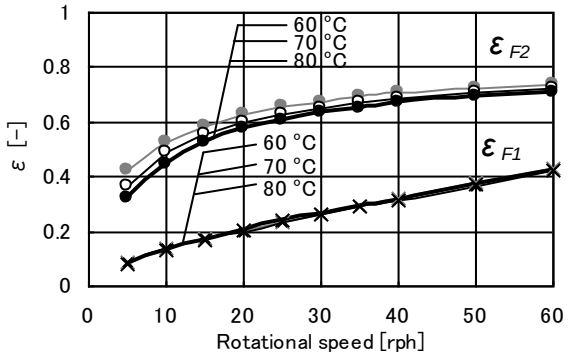

Fig. 11 Dehumidification effectiveness (1.0 m/s)

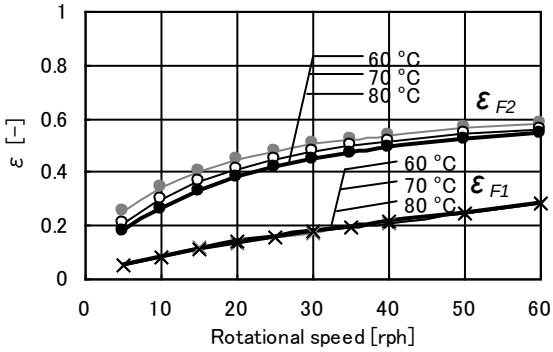

Fig. 12 Dehumidification effectiveness (2.0 m/s)

Nomenclature

ε: porosity (ratio of the air passage area to the cross-sectional area of a wheel) [-]
ρ_a: air density [kg/m^3] ρ_d: desiccant material density [kg_d/m^3] u: air velocity [m/s]
X_a: absolute humidity of flow passage air [kg-H_2O/kg-DA]
X_b: absolute humidity of desiccant material surface [kg-H_2O/kg-DA]
t: time [s] x: coordinate in the direction of the air passage axis [m]
λ_a': moisture conductivity of air [kg/{sm(kg-H_2O/kg-DA)}]
λ_d': moisture conductivity of desiccant material [kg/{sm(kg-H_2O/kg-DA)}]
γ: filling density of desiccant material (the mass of desiccant material per unit volume including the air passage) [kg_d/m^3]
w: moisture content (water vapor adsorption amount per unit mass of desiccant material) [kg-H_2O/kg_d]
α': moisture transfer coefficient on desiccant material surface [kg/{sm^2 (kg-H_2O/kg-DA)}]
α: heat transfer coefficient on desiccant material surface [J/(sm^2K)]
S: desiccant material surface area per unit volume including the air passage [m^2/m^3]
C_a: specific heat of air [J/(kgK)] C_d: specific heat of desiccant material [J/(kgK)]
θ_a: temperature of passage air [°C] θ_d: temperature of desiccant material [°C]
λ_a: thermal conductivity of air [J/(smK)]
λ_d: thermal conductivity of desiccant material [J/(smK)]
L: adsorption/desorption heat [J/kg]